
This is an electronic reprint of the original article.
This reprint may differ from the original in pagination and typographic detail.

Klemettinen, Lassi; Avarmaa, Katri; Taskinen, Pekka; Jokilaakso, Ari

Behavior of Nickel as a Trace Element and Time-Dependent Formation of Spinel in WEEE Smelting

Published in:
Extraction 2018

DOI:
[10.1007/978-3-319-95022-8_86](https://doi.org/10.1007/978-3-319-95022-8_86)

Published: 01/01/2018

Document Version
Peer reviewed version

Please cite the original version:

Klemettinen, L., Avarmaa, K., Taskinen, P., & Jokilaakso, A. (2018). Behavior of Nickel as a Trace Element and Time-Dependent Formation of Spinel in WEEE Smelting. In Extraction 2018: Proceedings of the First Global Conference on Extractive Metallurgy (pp. 1073-1082). (The Minerals, Metals & Materials Series). Springer International Publishing. https://doi.org/10.1007/978-3-319-95022-8_86

This material is protected by copyright and other intellectual property rights, and duplication or sale of all or part of any of the repository collections is not permitted, except that material may be duplicated by you for your research use or educational purposes in electronic or print form. You must obtain permission for any other use. Electronic or print copies may not be offered, whether for sale or otherwise to anyone who is not an authorised user.

Behavior of nickel as a trace element and time-dependent formation of spinels in WEEE smelting

Lassi Klemettinen, Katri Avarmaa, Pekka Taskinen, Ari Jokilaakso

All authors: Aalto University, School of Chemical Engineering, Department of Chemical and Metallurgical Engineering, P.O. Box 16200, Espoo, Finland

Lassi Klemettinen: M. Sc., lassi.klemettinen@aalto.fi, tel: +358 442149569

Katri Avarmaa: M. Sc., katri.avarmaa@aalto.fi, tel: +358 445619018

Pekka Taskinen: Prof. emer., pekka.taskinen@aalto.fi, tel: +358 405017411

Ari Jokilaakso: Prof., ari.jokilaakso@aalto.fi, tel: +358 503138885

Abstract

For better understanding and maximal value utilization of the WEEE smelting process, the behavior and distribution of different trace elements must be known. In this study, the behavior of nickel as a trace element was studied in an equilibrium system with metallic copper - spinel saturated iron silicate slag (with 3 wt-% K₂O) - iron aluminous spinel - gas. The experiments were conducted in alumina crucibles at 1300 °C, in oxygen pressure range of 10⁻¹⁰–10⁻⁵ atm. A time series of 15–60 min experiments was also conducted for investigating the formation rate of the primary spinel phase in the system. The results show that the distribution coefficient of nickel between metallic copper and liquid slag changes from approximately 70 to 0.4 along the increasing oxygen pressure range. In addition, a significant part of the nickel departs into the spinel phase. The spinel formation was investigated based on composition analysis results and visual observations from SEM-images.

Keywords: Distribution, Slag, Potassium oxide, Copper smelting

Introduction

One of the most viable options for treating crushed and sorted WEEE (Waste Electrical and Electric Equipment) copper scrap fractions is pyrometallurgical processing via black copper smelting [1, 2]. This process is followed by hydrometallurgical refining for recovering valuable or harmful trace elements from the produced copper alloy. For the recovery of trace elements, which preferentially distribute into the slag phase, some slag cleaning processes have been suggested and developed [3, 4, 5, 6]. A few integrated state-of-the-art factories, such as Umicore in Belgium, recover multiple elements from different material streams [7]. The base metal produced after the aforementioned process steps is copper, but the composition of the slag varies according to the raw materials and fluxes used. Alumina and potassium oxide are examples of slag components, which do not necessarily play a significant role in primary copper smelting, but may be present in considerable amounts when processing secondary raw materials, such as WEEE.

The behavior of different trace elements in secondary copper smelting conditions with high-alumina slags have not been very extensively studied, but a few studies have been published regarding for example precious metals and PGM's (platinum group metals) [8, 9, 10] and critical low-volume metals in electronics [11]. The present study continues to expand this knowledge by adding nickel to the list of trace metals investigated experimentally. When considering EEE, nickel is used for example in smart phones, tablets, CRT monitors, and LCD/LED notebooks [12], as well as different types of batteries (namely Li-ion and Ni-Cd) [13]. In different types of PCB's (Printed Circuit Boards), nickel represents 0.3–5.4 wt-% of the total mass [14]. Even though nickel is not as economically attractive as PGM's nor as scarce as indium for example, as its price is currently around two times that of copper (10.5 €/kg vs. 5.6 €/kg [15]), it is definitely worth recovering as we aim towards circular economy.

The behavior of nickel in copper-slag-gas systems with different types of slags has been studied to some extent previously. Takeda *et al.* [16] determined the distribution coefficient of nickel, among other trace elements, between metallic copper and calcium ferrite slags at different temperatures and oxygen pressures, and compared their results to those obtained with iron silicate slags [17]. Kaur *et al.* [18] studied the distribution of nickel between ferrous calcium silicate (FCS) slag and metallic copper (pO_2 10^{-6} atm, $T = 1300$ °C), and compared their results with calcium ferrite and iron silicate slags. Sukhomlinov & Taskinen [19] determined the distribution behavior of nickel between metallic copper and silica saturated iron silicate slag in pO_2 range of 10^{-8} – 10^{-4} atm, at 1300 °C. Reddy and Acholonu [20] investigated the distribution of nickel between Cu-Ni alloy and alumina-saturated iron silicate slag. Their experimental system was closer to the one employed in this paper, as the equilibrations were conducted in alumina crucibles, in pO_2 range of 10^{-10} – 10^{-8} atm, at 1300 °C.

The aim of this work was to investigate the distribution of nickel as a trace element in pyrometallurgical secondary copper processing conditions with iron-aluminous spinel saturated slags, with and without K_2O . Additional emphasis was placed on the formation of iron-aluminous spinel, which acts as the solid primary phase in the experimental system.

Experimental methods

Slag - copper alloy - gas equilibration experiments were performed in a vertical tube furnace (Nabertherm RHTV 120–150/18) equipped with $MoSi_2$ heating elements, Nabertherm P310 temperature controller and an alumina work tube (impervious pure alumina, 45/38 mm OD/ID). The temperature was measured with a calibrated Pt/Pt10 Rh thermocouple (Johnson-Matthey, accuracy ± 3 °C). The desired gas atmospheres in the work tube were obtained using CO/ CO_2 gas mixture (total flow rate 300 ml/min, STP), and these gases were flushed out between the experiments with nitrogen. Further details of the experimental set-up are presented in [21].

The copper alloy and slag were prepared from pure powders. The copper alloy mixture consisted of copper (99.999 %, Alfa Aesar) with 1 wt-% of Ni (99.996%, Alfa Aesar), Sn (99.85 %, Alfa Aesar), Sb (99.9 %, Alfa Aesar), and Te (99.99 %, Alfa Aesar). However, only the behavior of nickel as a trace element is presented in this article. The slag was mixed of SiO_2 (99.99%, Umicore) and Fe_2O_3 (99.99%, Alfa Aesar). Approximately 3 wt-% of K_2O (initially as K_2CO_3 , 99.5 %, Sigma-Aldrich) was added to the second slag mixture for studying the effect of potassium on the system. Fe/ SiO_2 ratio was 1.3 in the initial slag powder mixture. 200 mg of both copper and slag mixtures were weighed into alumina crucibles (Frialit AL23, 8/15 mm ID/H, respectively), which reacted with the system resulting in Al-Fe spinel saturation. The selected equilibration temperature was 1300 °C, equilibration time 16 h (confirmed with time series experiments of 8, 16 and 24 hours at oxygen pressure (pO_2) 10^{-6} atm), and the oxygen pressure range of interest from 10^{-10} to 10^{-5} atm. Duplicate experiments were conducted for both slag compositions in the pO_2 range of 10^{-9} – 10^{-6} atm, and these results have been included in the calculation of average values and standard deviations in Fig. 1–4.

The equilibrated-quenched samples were cast in epoxy resin and prepared for microanalysis with traditional dry polishing techniques. Analyses were conducted with SEM-EDS (Zeiss LEO 1450 Scanning electron microscope and Oxford Instruments X-Max 50 mm² Energy dispersive spectrometer) for determining whether the samples had reached equilibrium and observing the resulting microstructure. After SEM-EDS, the phase compositions were analyzed directly, phase-by-phase (copper alloy, liquid slag, solid spinel), with EPMA (Cameca SX-100 Electron Microprobe equipped with five Wavelength dispersive spectrometers). Eight analysis points were randomly taken from each phase for statistical reliability, and PAP-ZAF matrix correction procedure [22] was employed for raw data processing. The acceleration voltage was selected to be 20 kV, and the beam current 60 nA. For the copper alloy phase, a 100 μ m diameter electron beam was used. The slag phase was analyzed with a 50–100 μ m beam and the spinel with a 1 μ m beam, due to its small size and concentration gradient from the crucible side to the slag interface [11].

The standards used in EPMA analyses were hematite (O $K\alpha$ and Fe $K\alpha$), quartz (Si $K\alpha$), sanidine (K $K\alpha$), pentlandite (Ni $K\alpha$), alumina (Al $K\alpha$ for spinel, Al $K\beta$ for copper and slag), and copper (Cu $K\alpha$). Elemental detection limits were slightly different for each phase, as presented in Table 1. The detection limits were sufficient for detecting nickel in every phase in the entire oxygen pressure range investigated.

Table 1 Elemental detection limits in each phase with EPMA.

Element	O	Si	Al	K	Cu	Ni	Fe
Det. lim. (ppmw)							
- copper	1215	273	4497	116	348	107	179
- slag	1443	202	3258	94	278	95	197
- spinel	1365	193	183	92	272	92	195

Results

Fig. 1 (left side) shows the iron-to-silica ratio after equilibration as a function of oxygen partial pressure. The ratio was significantly reduced in all experimental conditions compared to the initial 1.3. The reason for this is mainly the formation of a spinel layer at the slag-crucible interface, which consumes a part of the iron. The composition of the spinel phase changes as a function of pO_2 , causing a decrease in the Fe/SiO₂ ratio in higher oxygen pressures. Moreover, the liquid domain and slag boundaries are significantly influenced by the increased dissolution of copper into the slag in higher oxygen pressures [11]. Basic oxides, in this case K₂O, increase the activity coefficient of iron in the slag, thus lowering its concentration. Therefore, the Fe/SiO₂ ratio is consistently lower in the K₂O containing slag.

The concentration of potassium oxide remained constant between 3.0–3.3 wt-% in the whole oxygen pressure range investigated. The changes in oxygen pressure did not alter the alumina concentration either, as shown in Fig. 1 (right side). Potassium oxide addition seems to decrease slightly the solubility of alumina into the slag.

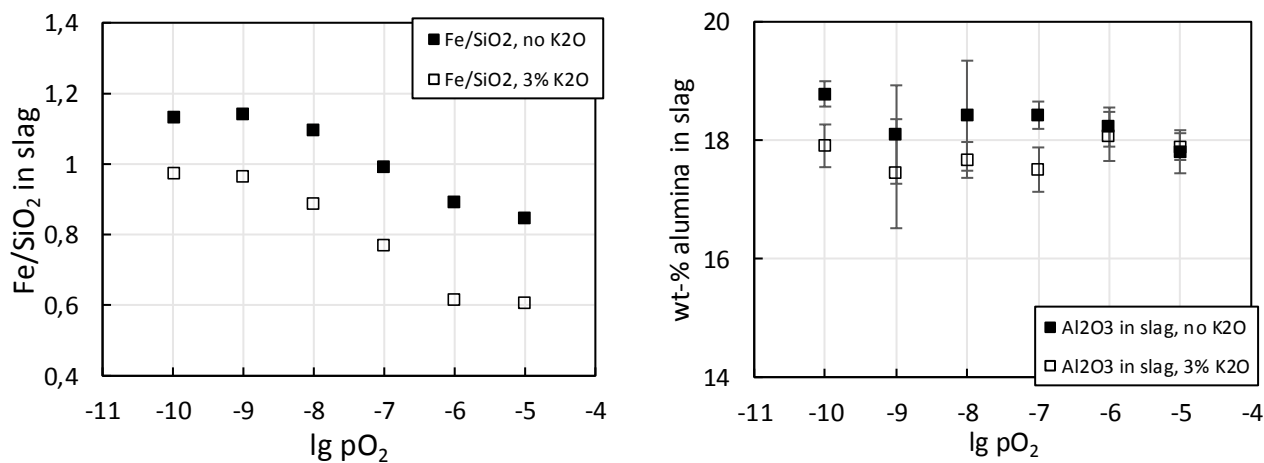


Fig. 1 Left: Iron-to-silica ratio in slags after 16 h equilibration as a function of oxygen pressure. The ratio in the starting material mixture was 1.3. Right: Alumina concentration in slags.

The concentrations of nickel in copper alloy and liquid slag are presented in Fig. 2 on the left and right side, respectively. As the oxygen pressure increases, nickel concentration decreases in the copper phase and increases in the slag phase. The increasing concentration of nickel in the spinel phase along the increasing oxygen pressure range is shown in Fig. 3 (left side). The concentration of nickel in the spinel is 2–4 times higher than copper concentration at lower pO_2 's, but copper dissolution becomes more dominant in oxidizing conditions. The total volume of the spinel phase in the system is difficult to estimate and, therefore, the extent of nickel vaporization at higher oxygen pressures is somewhat uncertain. However, it appears that even in the most oxidizing conditions, at least half of the original amount of nickel remains within the solid and liquid phases of the system based on the nickel concentrations in copper, slag and spinel.

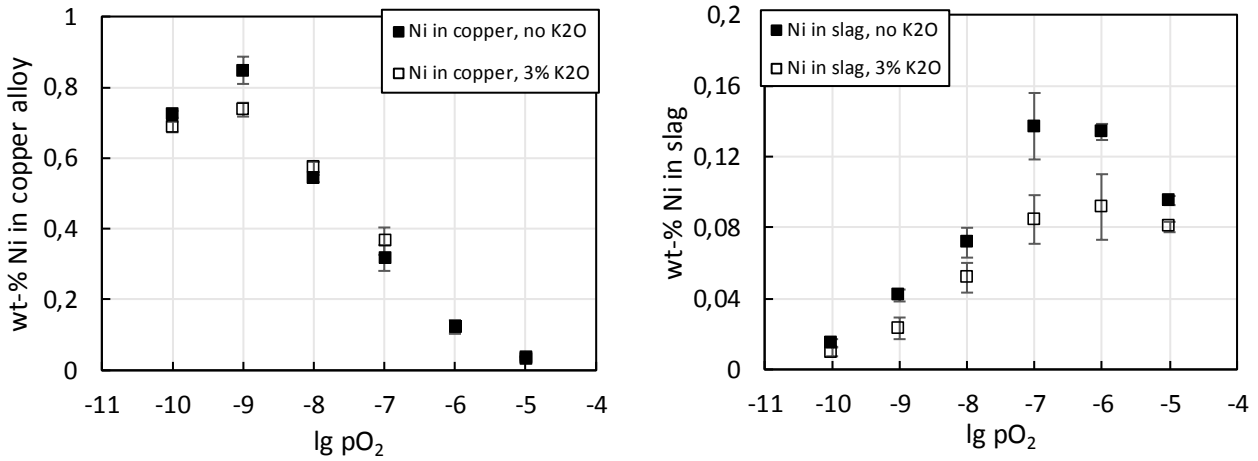


Fig. 2 Left: Nickel concentration in copper alloy. Right: Nickel concentration in slags.

The concentration of iron in the spinel phase increases significantly along the increasing oxygen pressure range, and the aluminum concentration decreases correspondingly, as depicted in Fig. 3 (right side). As the addition of K_2O decreases the iron concentration in the liquid slag phase, the spinel consequently becomes richer in iron. The spinel phase at the crucible-slag interface has a concentration gradient, and the areas adjacent to the liquid slag are in equilibrium with the copper-slag-gas system [11]. In oxidizing conditions (pO_2 10^{-7} – 10^{-5} atm), individual spinel grains surrounded by the slag also formed. Therefore, in experiments with reducing atmospheres, the spinel analyses were taken from the slag side of the edge spinel, and in oxidizing conditions from the spinels surrounded by liquid slag (i.e. slag spinels).

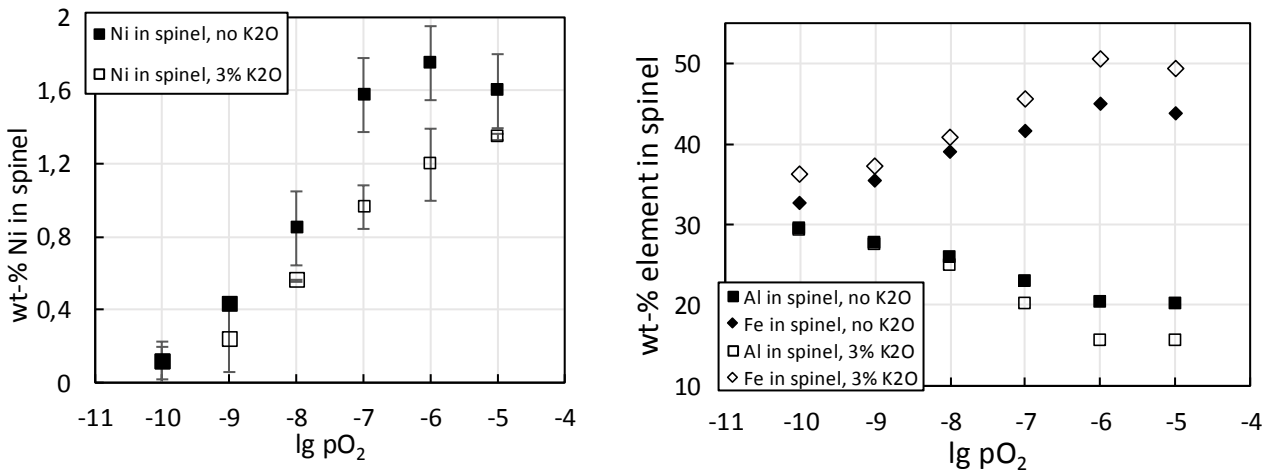


Fig. 3 Left: Nickel concentration in solid Al-Fe spinels. Right: Concentration of aluminum and iron in spinel phase as a function of oxygen pressure.

Discussion

The distribution of an element [Me] between two phases can be described with a thermodynamic parameter called distribution coefficient. This parameter can be expressed in its simplest form according to Equation (1):

$$L^{copper/slag} [Me] = \frac{[wt-\% Me]_{copper}}{(wt-\% Me)_{slag}} \quad (1)$$

Considering a typical equilibrium reaction (Equation 2) in copper-slag system, the distribution coefficient can also be written according to Equation (3):



$$\lg L^{copper/slag} [Me] = -\frac{x}{2} \lg pO_2 + \lg C \quad (3)$$

where [] and () brackets refer to metal and slag phases, respectively, and C includes the thermodynamic constants K , n_T and γ (equilibrium constant of reaction (2), number of moles in 100 g of alloy and slag, and the activity coefficients of the investigated metal and its oxide form). When plotting the logarithm of the distribution coefficient as a function of logarithm of the oxygen pressure, the oxidation state of the element in the slag phase can be determined from the slope of the experimental result points. The aforementioned plots for copper and nickel are presented in Fig. 4 left and right side, respectively. For copper, the distribution coefficient between copper alloy and slag decreases from approximately 90–100 in reducing conditions to 5 in most oxidizing conditions studied. As the distribution coefficient has constantly higher values with K₂O-containing slag, K₂O decreases copper losses into the liquid slag phase. The slope of the trend line fitted to the experimental points is -0.26 with both slags, which, according to Equation (3), indicates dissolution into the slag as a monovalent oxide Cu₂O. This result is in line with earlier observations [11, 21].

The distribution coefficient of nickel (Fig. 4 right side) decreases from approximately 50–70 in most reducing conditions of this study to 0.4 in oxidizing atmosphere. These values correspond quite well with the results of Kaur *et al.* [18] for FCS slags at pO_2 10⁻⁶ atm, and Sukhomlinov & Taskinen [19] for iron silicate slags in pO_2 range of 10⁻⁸–10⁻⁵ atm. Based on the results of this study, a slight decrease in nickel losses to the liquid slag phase can be obtained by changing the slag composition from silica saturated iron silicate slag to iron-aluminous spinel saturated slag. A more significant reduction is obtained with the addition of 3 wt-% K₂O. However, the considerable department of nickel into the solid spinel phase complicates the comparison regarding combined nickel losses.

The slope of the trend line for the distribution coefficient of nickel between copper alloy and slag is approximately -0.44 with both slags used in this study. This indicates dissolution into the slag as divalent oxide NiO, which agrees with the results of Takeda *et al.* and Kaur *et al.* [16, 18] obtained using calcium ferrite, FCS, and iron silicate slags. However, as the slope is slightly less negative than -0.5 (which corresponds to dissolution as NiO), nickel may dissolve both as Ni²⁺ and Ni⁰. This would agree with the observations of Reddy and Acholonu [20], although their distribution coefficient values were much higher than the ones obtained in this study.

For the recovery of nickel, distribution into the copper alloy phase is desirable. In reducing conditions, most of the nickel behaves in this manner. When the oxygen pressure increases, nickel starts to deport into the slag and spinel phases and, consequently, the concentration decreases in the alloy phase. For recovering nickel from the slag and spinel phases, the slag can be circulated back to earlier process steps [3], downstream pyrometallurgical processes [5], or possibly be treated with hydrometallurgical processes [4, 6].

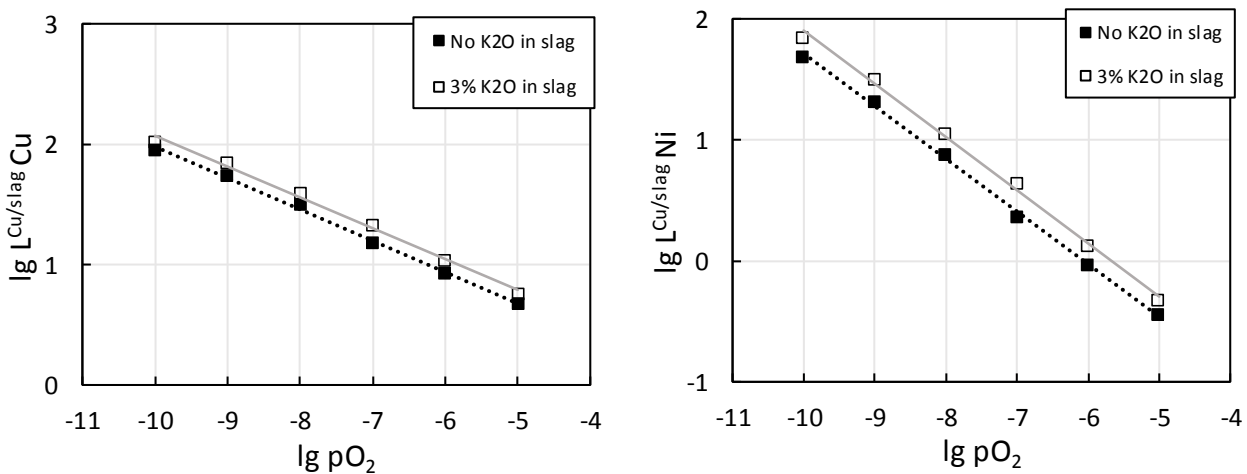


Fig. 4 Left side: Distribution coefficient of copper between copper alloy and liquid slags. Right side: Distribution coefficient of nickel between copper alloy and slags.

SEM-images of the spinel layer evolution at pO_2 10^{-8} atm with the 3 wt-% K_2O containing slag are shown in Fig. 5 a–d. After 15 minutes in 1300 °C, the copper alloy and slag phases are already completely molten, and the solid primary spinel phase has started forming. With increasing equilibration time, the spinel layer at the crucible-slag interface becomes more uniform. As Fig. 5 a–c show, the initial spinels appear brighter compared to the liquid slag. This phenomenon is referred to as the Z-contrast, which denotes the difference in the grey scale of the phases in an SEM-BSE (Backscattered Electron) image, related to the mean atomic number (Z) of the phase [23]. Phases with higher atomic number appear brighter compared to those with lower atomic number. When the system has reached equilibrium after 16 hours (Fig. 5 d), the difference in Z-contrast has evened out almost completely, indicating a similar average atomic number in the spinel and slag phases. The change in the atomic number contrast is explained in Fig. 6, which shows that the first spinel grains are preferentially comprised of iron oxides with very low concentration of aluminum. The dissolution of alumina into the liquid slag phase occurs through the spinel layer, and once the slag approaches saturation solubility regarding its alumina concentration, the aluminum concentration in the spinel phase begins to increase and the iron concentration decreases.

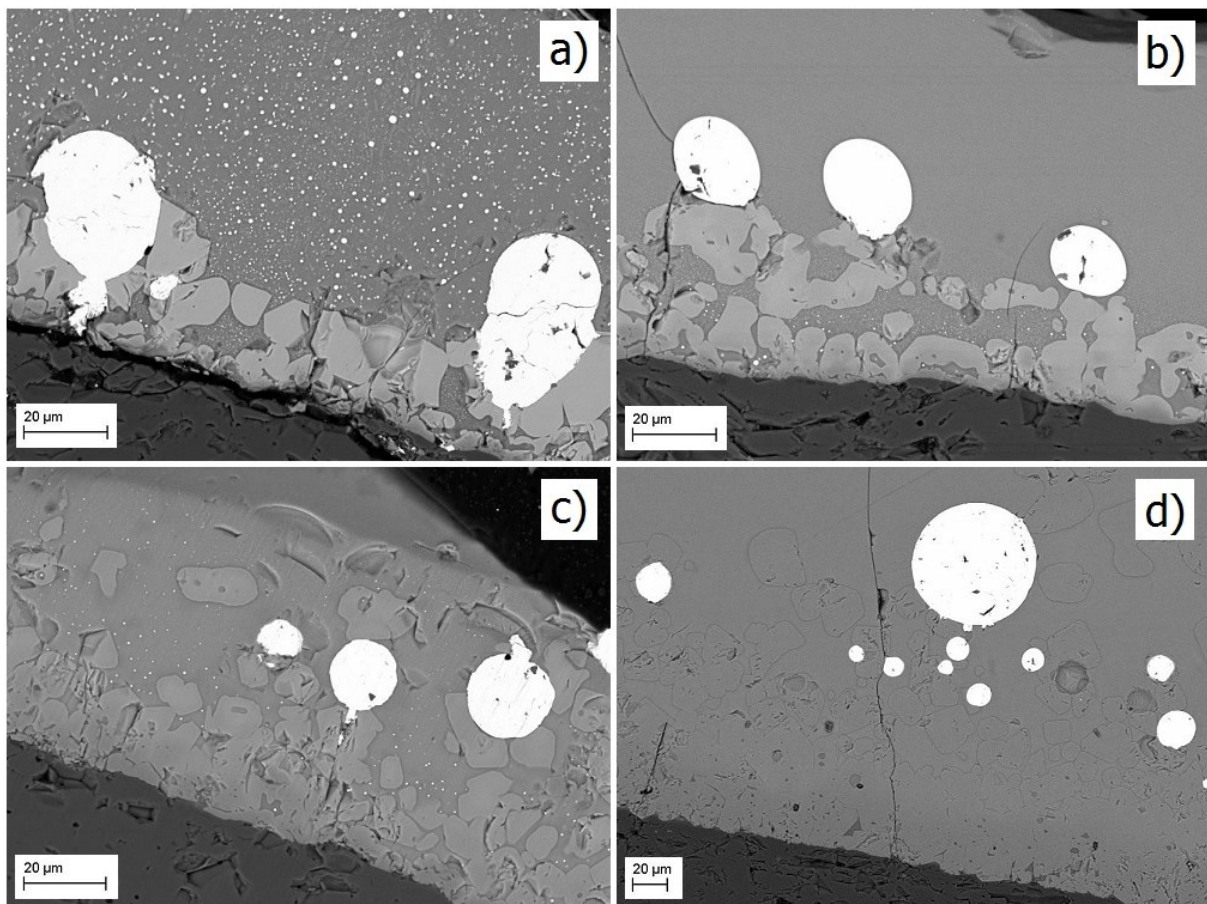


Fig. 5 SEM-BSE images of a) 15 min, b) 30 min, c) 60 min, d) 16 h equilibrated samples at pO_2 10^{-8} atm. The spinel layer on the crucible (dark grey at the bottom) – slag (grey) interface starts forming almost immediately after raising the sample to 1300 °C. When the equilibration time increases, the spinel becomes more uniform and the atomic number contrast difference compared to the slag decreases. After reaching equilibrium (Fig. 5 d), the spinel and slag have almost the same mean atomic number, and the spinel layer is very uniform. The brightest areas are copper alloy droplets.

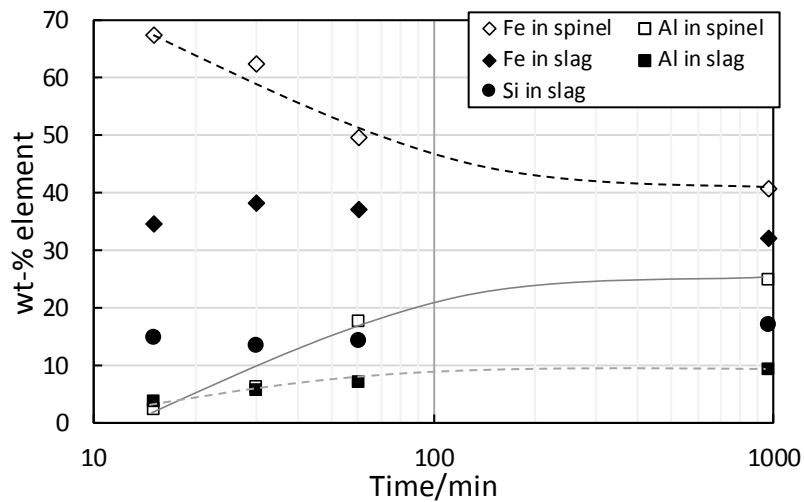


Fig. 6 Concentrations of Fe in spinel and slag, Si in slag, and Al in spinel and slag as a function of time. The slag contains 3 wt-% K_2O and the oxygen partial pressure is 10^{-8} atm.

Conclusions

This study investigated the behavior of nickel in secondary copper smelting conditions with K_2O -containing iron-aluminous spinel saturated slag. The results show that K_2O -addition decreases the losses of copper and nickel into the liquid slag phase. The formation of the solid iron-aluminous spinel is very rapid, and it dissolves a significant part of the nickel in oxidizing conditions. The results of this study expand the knowledge of trace element behavior in pyrometallurgical electronic scrap processing, and can be utilized in the industry to improve process control, as well as obtain more accurate slag chemistry models. The effect of K_2O addition on the slag boundaries and liquid domain will be investigated more closely in the future.

Acknowledgements

The scholarship from the Finnish Steel and Metal Producer's Fund (LK) has enabled this work. The assistance of Mr. Lassi Pakkanen at Geological Survey of Finland regarding the EPMA analyses is greatly appreciated.

References

- [1] Ghodrati M et al. (2016) Techno economic analysis of electronic waste processing through black copper smelting route. *Journal of Cleaner Production* 126:178–190
- [2] Wood J et al. (2011) Secondary Copper Processing using Outotec Ausmelt TSL Technology. Presented at the AusIMM's MetPlant conference, Perth, 2011
- [3] Piret NL (2000) Cleaning Copper and Ni/Co Slags: The Technical, Economic, and Environmental Aspects. *JOM* 52(8):18
- [4] Anand S, Kanta Rao P, Jena PK (1980) Leaching behaviour of copper converter slag in sulphuric acid. *Transactions of the Institution of Mining and Metallurgy* 33:77-81
- [5] Jones RT, Hayman DA, Denton GM (1996) Recovery of Cobalt, Nickel, and Copper from Slags, using DC-Arc Furnace Technology. Presented at the 35th Annual Conference of Metallurgists, Canada, 1996. Mintek Paper No. 8360

- [6] Anand S, Rao KS, Jena PK (1983) Pressure leaching of copper converter slag using dilute sulphuric acid for the extraction of cobalt, nickel and copper values. *Hydrometallurgy* 10:303-312
- [7] Hagelüken C (2006) Recycling of Electronic Scrap at Umicore's Integrated Metals Smelter and Refinery. *World of Metallurgy-ERZMETALL* 59(3):152-161
- [8] Avarmaa K, O'Brien H, Taskinen P (2016) Equilibria of gold and silver between molten copper and $\text{FeO}_x\text{-SiO}_2\text{-Al}_2\text{O}_3$ slag in WEEE smelting at 1300 °C. In: *Proceedings of the 10th International Conference on Molten Slags, Fluxes and Salts MOLTEN*, USA, 2016, 193-202
- [9] Nishijima W, Yamaguchi K (2014) Effects of Slag Composition and Oxygen Potential on Distribution Ratios of Platinum Group Metals between $\text{Al}_2\text{O}_3\text{-CaO-SiO}_2\text{-Cu}_2\text{O}$ Slag System and Molten Copper at 1723 K. *Journal of the Japan Institute of Metals* 78(7):267-273
- [10] Klemettinen L, Avarmaa K, Taskinen P (2017) Trace Element Distribution in Black Copper Smelting. *World of Metallurgy – ERZMETALL* 70(5):257-264
- [11] Avarmaa K, Yliaho S, Taskinen P (2018) Recoveries of rare elements Ga, Ge, In and Sn from waste electric and electronic equipment through secondary copper smelting. *Waste Management* 71:400-410
- [12] Cucchiella F et al. (2015) Recycling of WEEE's: An economic assessment of present and future e-waste streams. *Renewable and Sustainable Energy Reviews* 51:263-272
- [13] Zhang L, Xu Z (2016) A review of current progress of recycling technologies for metals from waste electrical and electronic equipment. *Journal of Cleaner Production* 127:19-36
- [14] Duan H et al. (2011) Examining the technology acceptance for dismantling of waste printed circuit boards in light of recycling and environmental concerns. *Journal of Environmental Management* 92(3):392-399
- [15] London Metal Exchange, 3-month average prices, checked January 25, 2018. <https://www.lme.com/Metals>
- [16] Takeda Y, Ishiwata S, Yazawa A (1983) Distribution Equilibria of Minor Elements between Liquid Copper and Calcium Ferrite Slag. *Transactions of the Japan Institute of Metals* 24(7):518-528
- [17] Kashima M, Eguchi M, Yazawa A (1978) Distribution of Impurities between Crude Copper, White Metal and Silica-Saturated Slag. *Transactions of the Japan Institute of Metals* 19:152-158
- [18] Kaur RR, Swinbourne DR, Nexhip C (2009) Nickel, lead and antimony distributions between ferrous calcium silicate slag and copper at 1300 °C. *Mineral Processing and Extractive Metallurgy* 118(2):65-72
- [19] Sukhomlinov D, Taskinen P (2017) Distribution of Ni, Co, Ag, Au, Pt, Pd between Copper Metal and Silica Saturated Iron Silicate Slag. In: *Proceedings of the European Metallurgical Conference EMC*, Germany, 2017, 3:1029-1038
- [20] Reddy R.G, Acholonu CC (1984) Distribution of Nickel between Copper-Nickel and Alumina Saturated Iron Silicate Slags. *Metallurgical Transactions B* 15B:33-37
- [21] Klemettinen L, Avarmaa K, Taskinen P (2017) Slag Chemistry of High-Alumina Iron Silicate Slags at 1300 °C in WEEE Smelting. *Journal of Sustainable Metallurgy* 3:772-781
- [22] Pouchou JL, Pichoir F (1986) Basic expression of "PAP" computation for quantitative EPMA. In: *11th international congress on X-ray optics and microanalysis ICXOM*, Canada, 1986, 249-256
- [23] Lloyd GE (1987) Atomic number and crystallographic contrast images with the SEM: a review of backscattered electron techniques. *Mineralogical Magazine* 51:3-19